

Ab initio estimates of the Curie temperature for magnetic compounds

This article has been downloaded from IOPscience. Please scroll down to see the full text article.

2006 J. Phys.: Condens. Matter 18 9795

(<http://iopscience.iop.org/0953-8984/18/43/003>)

View [the table of contents for this issue](#), or go to the [journal homepage](#) for more

Download details:

IP Address: 130.63.180.147

The article was downloaded on 04/08/2013 at 08:15

Please note that [terms and conditions apply](#).

***Ab initio* estimates of the Curie temperature for magnetic compounds**

J Kübler

Institut für Festkörperphysik, Technische Universität, Darmstadt, Germany

E-mail: jkubler@fkp.tu-darmstadt.de

Received 24 July 2006, in final form 27 September 2006

Published 13 October 2006

Online at stacks.iop.org/JPhysCM/18/9795

Abstract

The local spin-density functional approximation is increasingly being used for materials applications such as predicting structural and magnetic properties. The recently acquired ability to model low-lying magnetic excitations like magnons is used for deriving useful formulae to estimate the Curie (Néel) temperatures of magnetic compounds. Underlying this is Moriya's unified approach, appropriately formulated for density functional use. The theory is applied to the classical compounds FeNi, CoNi, FeNi₃, CoNi₃, and RhMn₃ to establish a level of confidence, and to the Heusler compounds NiMnSb, Mn₂VAl, Co₂FeSi, Mn₃Al, and Mn₃Ga, which are presently studied with possible applications in mind for advanced spin electronic devices.

1. Introduction

The magnetism of the metallic compounds to be considered here is due to itinerant electrons. The theory to treat these with has traditionally been pursued along two different directions, in fact until recently by two separate communities: one uses model Hamiltonians, most prominently the Hubbard model [1], in conjunction with powerful many-body techniques [2]; the other uses density functional theory and its local spin-density functional approximation (LSDA). In contrast to the former, the latter is an *ab initio* approach which does not require empirical parameters as input [3]. Although it appears that the two main streams are about to merge into one (see, for instance, Lichtenstein *et al* [4]), practical and quick predictions of magnet properties of metals can only be obtained by an *ab initio* approach like the LSDA.

Itinerant electrons can cooperate in forming localized magnetic moments in some compounds and completely delocalized (and weak) moments in others. The Rhodes–Wohlfarth plot [5] provides an empirical viewpoint for a large range of cases, from very weak ferromagnets to the local moment limit. The latter is traditionally treated by the venerable Heisenberg model, which is also useful in the framework of the LSDA. The other limit of weak ferromagnets has been attacked by using the Ginzburg–Landau model [6, 7], which is a model that can also be applied to *ab initio* calculations, as done e.g. for ZrZn₂ [8]. Moriya [9] describes

an attempt to cover the whole range. It will be shown to what extent Moriya's model can be used for reliable estimates of the Curie (Néel) temperature for ferromagnets, ferrimagnets and antiferromagnets by means of *ab initio* calculations in the LSDA. Such estimates are needed to complete modern predictions of 'tailored' magnetic properties of materials such as that of Wurmehl *et al* [10].

Some of the itinerant-electron magnets chosen here as examples (NiMnSb, Mn₂VAl, Co₂FeSi, and Mn₃Ga) possess both local and less localized moments. They are not part of the Rhodes–Wohlfarth plot. This classification stems from the Heusler compounds, where the type of localization was first described [11, 12]. The moments of other selected compounds like the ferromagnets FeNi, CoNi, CoNi₃ and the non-collinear antiferromagnet RhMn₃ are intermediate.

Although density-functional theory [13]—together with well-known approximations like the LSDA—is a ground-state theory, it is possible to apply the LSDA for modelling the energies of low-lying excited states. One approach suitable for studying magnetic excitations is based on spin spiral configurations for the magnetic moments, as was done in earlier work [14] to [17] as well as [8] (and references given therein). The basis for this approach is summarized briefly in the next section. This is followed by a derivation and discussion of a simple expression for the Curie temperature—or the Néel temperature, respectively—of metallic compounds in the spherical approximation starting from a functional integral gleaned from the work of Moriya [9]. The formula derived requires the evaluation of exchange as a function of the wavevector which can be performed by computing total energies. These exchange functions depend on the type of crystal structure, or put differently, on the number of sublattices, different structures giving rise to different expressions. These are derived for a number of cases and are evaluated numerically in the LSDA for FeNi, CoNi, FeNi₃, CoNi₃, NiMnSb, Mn₂VAl, Co₂FeSi, Mn₃Al, Mn₃Ga, and RhMn₃ in the last section, where the results are put into context and discussed.

2. Theory

2.1. Spin spirals

A spiral magnetic structure is defined by giving the Cartesian coordinates of the magnetization vector, $\mathbf{M}_{n\tau}$, as

$$\mathbf{M}_{n\tau} = M_\tau [\cos(\mathbf{q} \cdot \mathbf{R}_n + \varphi_\tau) \sin \theta_\tau, \sin(\mathbf{q} \cdot \mathbf{R}_n + \varphi_\tau) \sin \theta_\tau, \cos \theta_\tau]. \quad (1)$$

Here \mathbf{q} is the wavevector that characterizes the spiral and M_τ is the magnitude of the magnetic moment at site $\mathbf{R}_n + \boldsymbol{\tau}$, where \mathbf{R}_n is a translation and $\boldsymbol{\tau}$ a basis vector; φ_τ and θ_τ are polar angles.

Since all atoms of the spiral structure separated by a translation \mathbf{R}_n are equivalent, possessing magnetic moments of equal magnitude, periodicity is not lost with respect to lattice translations. This leads to a useful property for the single-particle spinor functions, which is embodied in a generalized Bloch theorem:

$$\{\mathbf{q} \cdot \mathbf{R}_n | \epsilon | \mathbf{R}_n \} \psi_{\mathbf{k}}(\mathbf{r}) = e^{i\mathbf{k} \cdot \mathbf{R}_n} \psi_{\mathbf{k}}(\mathbf{r}), \quad (2)$$

where the $\psi_{\mathbf{k}}(\mathbf{r})$ are eigenspinors. The operator $\{\mathbf{q} \cdot \mathbf{R}_n | \epsilon | \mathbf{R}_n \}$ combines a lattice translation \mathbf{R}_n and the identity space rotation, denoted by the identity symbol ϵ , with a spin rotation about the z -axis by an angle $\mathbf{q} \cdot \mathbf{R}_n$. The vectors \mathbf{k} lie in the first Brillouin zone, which is defined in the usual way. The spin spiral defined in (1) does not break the translational symmetry of the lattice. This statement is independent of the choice of \mathbf{q} which, therefore, need not be commensurate with the lattice. A practical consequence is that no supercell is needed to solve the Schrödinger

equation in the presence of spin spirals. From a representation of the generalized translation operator, which is easily obtained from the spin-1/2 rotation matrix as

$$\{\mathbf{q} \cdot \mathbf{R}_n | \in |\mathbf{R}_n\rangle\} \psi(\mathbf{r}) = \begin{pmatrix} \exp(i\mathbf{q} \cdot \mathbf{R}_n/2) & 0 \\ 0 & \exp(-i\mathbf{q} \cdot \mathbf{R}_n/2) \end{pmatrix} \psi(\mathbf{r} - \mathbf{R}_n) \quad (3)$$

one can see that the spiral wavevector \mathbf{q} is chosen from inside the first Brillouin zone; \mathbf{q} -vectors outside give nothing new. The original derivation of the properties of the spin spiral is due to Herring [18]. This was rediscovered independently and put to use by Sandratskii [19] and [15]. It should be emphasized that, in order to apply this concept, spin-orbit coupling must be negligibly small.

If the Kohn–Sham Schrödinger equation that must be solved in the LSDA is written in the usual form as $\mathcal{H}_\mathbf{q}\psi = \varepsilon\psi$, then the Hamiltonian, $\mathcal{H}_\mathbf{q}$, can be specified in the following form [15]:

$$\mathcal{H}_\mathbf{q} = -\mathbf{1}\nabla^2 + \sum_{n\tau} \Theta(|\mathbf{r}_{n\tau}|) U^+(\theta_\tau, \varphi_\tau, \mathbf{q}) \begin{pmatrix} v_+^{\text{eff}}(|\mathbf{r}_{n\tau}|) & 0 \\ 0 & v_-^{\text{eff}}(|\mathbf{r}_{n\tau}|) \end{pmatrix} U(\theta_\tau, \varphi_\tau, \mathbf{q}) \quad (4)$$

where $|\mathbf{r}_{n\tau}| = |\mathbf{r} - \mathbf{R}_n - \boldsymbol{\tau}|$, $\Theta(|\mathbf{r}_{n\tau}|)$ is the unit step function that vanishes outside the atomic sphere centred at $|\mathbf{R}_n + \boldsymbol{\tau}|$, the indices $+$ and $-$ label the spin-up and spin-down effective Kohn–Sham potential, and $U(\theta, \varphi, \mathbf{q}) \doteq U(\theta, \mathbf{q} \cdot \mathbf{R} + \varphi)$ is the spin-1/2 rotation matrix.

An important observation is that the Hamiltonian above depends on a parameter \mathbf{q} , the wavevector characterizing the spin spiral. Niu and Kleinman [20] showed that, just like the adiabatic approximation for decoupling the electronic from the ionic motion in solids, this parameter will lead to a Berry phase. In fact they demonstrated [20, 21] that the Berry curvature involved in the equation of motion describes how the total spin component along the symmetry axis changes due to spin deviations from the ground-state configuration. So if the total energy is calculated by constraining the magnetic moment to the ground-state value M for a small value of θ , then the spin wave energy for an itinerant electron ferromagnet is (in atomic units) given by

$$\omega(\mathbf{q}) = \lim_{\theta \rightarrow 0} \frac{4}{M} \frac{E(\mathbf{q}, \theta)}{\sin^2 \theta}, \quad (5)$$

where the total energy $E(\mathbf{q}, \theta)$ is counted from the ground-state value. Since the total energy is nearly proportional to $\sin^2 \theta$, the choice of θ is not very critical. This formula not only establishes the spiral energy as a physical quantity but has also been shown to lead to very good agreement with measured magnon energies for Fe, Co and Ni [16]. Thus one can assume with a great deal of confidence that the adiabatic approximation is valid for these spin systems. The spiral energy, furthermore, is the central quantity for estimating the Curie or Néel temperature of metallic compounds, as will be shown next.

2.2. Thermodynamics: the spherical approximation

A useful theory that, in principle, applies to the entire range of cases from very weak ferromagnets to the local moment limit was proposed by Moriya and Takahashi [22] (Moriya, chapters 7–8, [9]) who used the Stratonovich–Hubbard functional integral method. One can construct a simple form for the functional that does not contain the original model parameters. Instead one can formulate the appropriate functional in terms of on-site and off-site total energies obtainable in the LSDA. In a notation somewhat different from that of Moriya and Takahashi, the formalism is quite general and may be described as follows.

A functional $\Psi = \Psi(M_\tau, \mathcal{L}_\tau, \mathbf{M}_{n\mathbf{q}})$ is constructed that depends on the magnetization of atom τ , M_τ , the size of the local moment of atom τ , \mathcal{L}_τ , and the fluctuation vector

$\mathbf{M}_{n\mathbf{q}} = (m_{xn\mathbf{q}}, m_{yn\mathbf{q}}, m_{zn\mathbf{q}})$ of the ‘normal mode’ labelled n . The functional integral to be evaluated is then

$$\exp(-F/k_B T) \propto \prod_{\tau} \int d\mathcal{L}_{\tau}^2 \int \prod_{n\mathbf{q}} d\mathbf{M}_{n\mathbf{q}} \exp[-\Psi(M_{\tau}, \mathcal{L}_{\tau}, \mathbf{M}_{n\mathbf{q}})/k_B T] \quad (6)$$

which supplies the free energy, F . The normal modes are given by the eigenvectors $\{C_{n\tau}\}$ to be obtained by diagonalizing an exchange matrix that will be discussed subsequently. In writing down an expression for the functional Ψ , one uses an important approximation in which Lagrange multipliers, $\lambda_{\alpha\tau}$, for each cartesian component, ($\alpha = x, y, z$), constrain the size of the magnetic moments to be near a most probable size. This is called the *spherical approximation*. Thus one writes

$$\begin{aligned} \Psi = & \sum_{\tau\tau'} \sum_{\mathbf{q}n} j_{\tau\tau'}(\mathbf{q}) C_{n\tau}^* C_{n\tau'} |\mathbf{M}_{n\mathbf{q}}|^2 + \sum_{\tau} E_{\tau}(M_{\tau}, \mathcal{L}_{\tau}^2) \\ & - \sum_{\alpha\tau} \lambda_{\alpha\tau} \left(\mathcal{L}_{\alpha\tau}^2 + \delta_{\alpha z} M_{\tau}^2 - \sum_{n\mathbf{q}} |C_{n\tau}|^2 |m_{\alpha n\mathbf{q}}|^2 \right). \end{aligned} \quad (7)$$

Here $j_{\tau\tau'}(\mathbf{q})$ is the exchange energy as a function of the wavevector \mathbf{q} that accounts for the off-site interactions, whereas $E_{\tau}(M_{\tau}, \mathcal{L}_{\tau}^2)$ is the on-site energy of a given configuration of local moments and magnetization.

The integral over $\mathbf{M}_{n\mathbf{q}}$ can now be carried out, however the $\mathbf{q} = 0$ component $\mathbf{M}_{\tau\mathbf{q}=0} = (0, 0, m_{\tau z0}) = (0, 0, M_{\tau})$ is singled out and identified as the macroscopic magnetization of atom τ . The result is

$$\begin{aligned} \exp(-F/k_B T) \propto & \int d\mathcal{L}_{\tau}^2 \int dM_{\tau} \\ & \times \exp \left\{ -\frac{\sum_{\tau} [E_{\tau}(M_{\tau}, \mathcal{L}_{\tau}^2) - \sum_{\alpha} \lambda_{\alpha\tau} \mathcal{L}_{\alpha\tau}^2]}{k_B T} - \frac{1}{2} \sum_{\alpha n\mathbf{q}} \ln \frac{\lambda_{\alpha n} + j_n(\mathbf{q})}{\pi k_B T} \right\}. \end{aligned} \quad (8)$$

Here the diagonalized exchange function is defined by

$$j_n(\mathbf{q}) = \sum_{\tau\tau'} j_{\tau\tau'}(\mathbf{q}) C_{n\tau}^* C_{n\tau'}. \quad (9)$$

Furthermore

$$\lambda_{\alpha n} = \sum_{\tau} \lambda_{\alpha\tau} |C_{n\tau}|^2 \quad (10)$$

and

$$M_{\tau}^2 = \sum_{n\alpha} |C_{n\tau}|^2 |m_{\alpha n\mathbf{q}=0}|^2. \quad (11)$$

Next, equation (8) is differentiated with respect to $\lambda_{\alpha\tau}$ and the result is equated to zero in order to determine the condition for the constraint that is implied by the spherical approximation. With $\mathcal{L}_{\tau}^2 = \sum_{\alpha=1}^3 \mathcal{L}_{\alpha\tau}^2$ and $\sum_{\tau} |C_{n\tau}|^2 = 1$, one obtains for the local moment

$$\sum_{\tau} \mathcal{L}_{\tau}^2 = \frac{k_B T}{N} \sum_{\alpha} \sum_{\mathbf{q}n} \chi_{\alpha n}(\mathbf{q}), \quad (12)$$

where

$$\chi_{\alpha n}(\mathbf{q}) = 1/[2\lambda_{\alpha n} + 2j_n(\mathbf{q})]. \quad (13)$$

It is emphasized that, for simplicity in writing, thermally averaged quantities and the original variables are not distinguished in the notation used here. Next, a saddle-point approximation is

employed to evaluate the integral over \mathcal{L}_τ . The saddle-point condition is obtained by taking the derivative with respect to $\mathcal{L}_{\alpha\tau}^2$. This gives

$$\lambda_{\alpha\tau} = \frac{\partial E_\tau(M_\tau, \mathcal{L}_\tau^2)}{\partial \mathcal{L}_{\alpha\tau}^2} + \frac{k_B T}{N} \sum_{\mathbf{q}n} \chi_{\alpha n}(\mathbf{q}) \frac{\partial j_n(\mathbf{q})}{\partial \mathcal{L}_{\alpha\tau}^2}. \quad (14)$$

The quantity $\chi_{\alpha n}(\mathbf{q})$ in (12) is identified as the susceptibility using the fluctuation-dissipation theorem in the static approximation.

Attention is now limited to temperatures above the ordering temperature where $M_\tau = 0$ for all basis atoms τ . Then, because of isotropy, equation (12) becomes

$$\sum_\tau \mathcal{L}_\tau^2 = \frac{3k_B T}{N} \sum_{\mathbf{q}n} \chi_n(\mathbf{q}), \quad (15)$$

where, from (13), the susceptibility is

$$\chi_n(\mathbf{q}) = 1/[2\lambda_n + 2j_n(\mathbf{q})]. \quad (16)$$

Using $\lambda_n = \sum_\tau \lambda_\tau |C_{n\tau}|^2$, the quantity λ_n is to be determined with

$$\lambda_\tau = 3 \frac{\partial E_\tau(0, \mathcal{L}_\tau^2)}{\partial \mathcal{L}_\tau^2} + 3 \frac{k_B T}{N} \sum_{\mathbf{q}n} \chi_n(\mathbf{q}) \frac{\partial j_n(\mathbf{q})}{\partial \mathcal{L}_\tau^2}. \quad (17)$$

At the Curie (Néel) temperature, the first term on the right-hand side vanishes. Then, ignoring the second term, one sees that $\lambda_n = 0$ for all n . Thus the Curie temperature in the spherical approximation is obtained as

$$k_B T_c^{\text{SP}} = \frac{2}{3} \sum_\tau \mathcal{L}_\tau^2 \left[\frac{1}{N} \sum_{\mathbf{q}n} \frac{1}{j_n(\mathbf{q})} \right]^{-1}. \quad (18)$$

At this stage, however, the size of the local moment, \mathcal{L}_τ , is not known unless one succeeds in solving equations (15) to (17) self-consistently. A number of comments are in order.

For the case of a primitive lattice, one might assume $\mathcal{L}^2 = S(S+1)$; equation (18) with this choice is then known as the RPA formula, which can be derived quantum mechanically for a spin- $S = 1/2$ system, for which $\mathcal{L}^2 = S(S+1)$ [23–25]. For itinerant-electron systems, however, a relation in terms of S is not defined. In spite of this, in many applications of the RPA formula one simply takes $\mathcal{L}^2 = M_0^2$, where M_0 is the saturation magnetization. For the case of non-primitive lattices, equation (18) is new as far as the sum on the local moments squared is concerned.

More insight is obtained if equations (15) to (17) are solved. Assuming that the exchange functions $j_n(\mathbf{q})$ and the on-site energy $E_\tau(0, \mathcal{L}_\tau^2)$ are known, then \mathcal{L}_τ^2 and the uniform susceptibility $\chi_{0n}^{-1} = 2\lambda_n$ can in principle be obtained in terms of the temperature.

For the total energy $E_\tau(0, \mathcal{L}_\tau^2)$, one is tempted to use the fixed spin method (FSM) first employed by Schwarz and Mohn [26]. This method gives the total energy as a function of the magnetization, which can then be expanded in powers of the magnetic moment. Once the expansion coefficients are known, it is easy to include fluctuations. This has been done before [7, 8, 14, 27], but it is found that the expansion coefficients are too large and must be renormalized [8, 28]. The reason for the failure of the FSM is that this representation of the total energy is only accurate near the minimum of the total energy where the moment is almost fully developed; when the magnetization is small, the disordered local moment state [3] is more appropriate, but not easy to treat with the FSM.

If the expansion obtained by the FSM is renormalized and the total energy is written as a Landau expansion, the Curie temperature thus obtained is smaller than the spherical

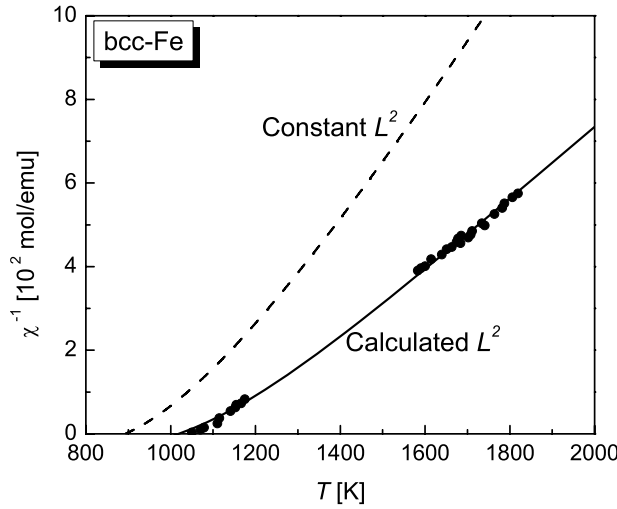


Figure 1. Calculated inverse susceptibility of iron. The dashed curve is the inverse susceptibility in the spherical approximation with constant \mathcal{L}^2 ; the solid curve is obtained by solving (15) to (17) self-consistently for the case of a primitive lattice. Dots are the experimental data from Shimizu [29].

approximation by a factor of 3/5. This is often called the *spin-fluctuation approximation*, which is thought to be a good starting point for weak ferromagnets.

To demonstrate that, for the case of a nearly localized ferromagnet, the formalism can approximately be exploited to calculate the local moment together with the Curie–Weiss law for the susceptibility, one may assume that, for this case, an expansion of the energy function $E(0, \mathcal{L}^2)$ about the value of $\mathcal{L}^2/M_0^2 = 1$ is meaningful. The derivative of the exchange function with respect to \mathcal{L}^2 in (17) can then be estimated from $\partial j(\mathbf{q})/\partial M_0^2$, i.e. replacing \mathcal{L} by M_0 . The latter derivative has been obtained numerically by finite differences using constrained total energy calculations to values of the magnetic moment, $M_0 \pm \Delta M$, for bcc-Fe.

Employing the expansion—which should not be confused with the FSM—

$$E(0, \mathcal{L}^2) = \frac{1}{4} \chi_{\text{eff}}^{-1} \cdot (\mathcal{L}^2/M_0^2 - 1), \quad (19)$$

the result shown in figure 1 for the inverse susceptibility for bcc-Fe is obtained. The value used here for the expansion coefficient is $\chi_{\text{eff}} \simeq 0.67 \times 10^{-4} \text{ emu mol}^{-1}$. The Curie temperature is obtained as $T_c = 1018 \text{ K}$, which is to be compared with the experimental value of 1044 K. The magnetic moment at the calculated Curie temperature is calculated to be $\mathcal{L} \simeq 1.07 M_0$. It should be stressed that the only input parameter is χ_{eff} which, together with the *ab initio* exchange function $j(\mathbf{q})$, explains both the slope and the Curie temperature. It is interesting to observe that χ_{eff} is of the order of magnitude of a Brillouin-zone average of the non-uniform susceptibility $\chi(\mathbf{q})$ [15]. The agreement with the experimental data is perhaps fortuitous.

This section is closed with a remark about the mean-field approximation (MFA) for the multi-sublattice case which is of interest here. A classical review article is that by Anderson [30] and, of the many modern applications of the MFA which use the LSDA, only the recent paper by Sasioglu *et al* [17] is mentioned here for brevity.

The MFA for the multi-sublattice case is obtained by including the $T = 0$ magnetic moments in the definition of the exchange constants, i.e. $J_{\tau\tau'}(\mathbf{q}) \doteq M_\tau j_{\tau\tau'}(\mathbf{q}) M_{\tau'}$. The summed exchange $(1/N) \sum_{\mathbf{q}} J_{\tau\tau'}(\mathbf{q})$ represents the mean field at site τ due to site τ' and is then diagonalized, the largest eigenvalue, J_{max} , determining the Curie temperature in the

MFA [30]:

$$k_B T_c^{\text{MF}} = (2/3) J_{\text{max}}. \quad (20)$$

2.3. Exchange in detail

To calculate the exchange functions, $j_{\tau\tau'}(\mathbf{q})$, one starts with the off-site total energy, $E_{\text{OS}}(\mathbf{q})$, which is written by means of spin spirals in the following way:

$$E_{\text{OS}}(\mathbf{q}) = \sum_{\tau\tau'} M_\tau M_{\tau'} [j_{\tau\tau'}(\mathbf{q}) \sin \theta_\tau \sin \theta_{\tau'} \cos(\varphi_\tau - \varphi_{\tau'}) + j_{\tau\tau'}(0) \cos \theta_\tau \cos \theta_{\tau'}], \quad (21)$$

where M_τ , θ_τ and φ_τ are the polar coordinates for the magnetic moment vector of atom τ . The total energy is now computed using the force theorem [31, 32], i.e. the band energies are summed up to the Fermi energy for a given spin configuration using, for these calculations, the self-consistent ground-state potentials. Throughout, equation (18) is now used with the substitution $\mathcal{L}_\tau^2 = M_\tau^2$, where M_τ is the magnetic moment (saturation moment) of atom τ . The numerical work done in this paper was carried out with the ASW method [33], where the atomic sphere approximation is used for the construction of the effective crystal potential and the von Barth-Hedin [34] approximation for exchange and correlation.

2.3.1. Two magnetic atoms per cell. For the case of two magnetic atoms in the unit cell (two sublattices), such as FeNi, CoNi, and NiMnSb, one determines the three functions $j_{11}(\mathbf{q})$, $j_{22}(\mathbf{q})$, and $j_{12}(\mathbf{q})$ by calculating band energies scanning the BZ four times using the usual special q -points. First one chooses $\theta_1 = \theta_2 = \theta$ and all azimuthal angles equal to zero, calling the resulting energy $e_0(\mathbf{q})$. Next the azimuthal angle is chosen to be $\varphi = \mathbf{q} \cdot \boldsymbol{\tau}$ and the result is denoted by $e_1(\mathbf{q})$. A third scan results in the energy $e_2(\mathbf{q})$ where the sign of the term $\cos(\mathbf{q} \cdot \boldsymbol{\tau})$ is changed with a choice of a reciprocal lattice vector obeying $\mathbf{K} \cdot \boldsymbol{\tau} = \pi$. Here one uses the fact that the exchange functions are periodic in reciprocal space. A last scan is carried out with $\theta_1 = 0$ and $\theta_2 = \theta$ denoting the energy by $e_3(\mathbf{q})$. The desired exchange functions can now be determined by subtracting the energy origin

$$e_0(\mathbf{q} = 0) = M_1^2 j_{11}(0) + M_2^2 j_{22}(0) + 2M_1 M_2 j_{12}(0). \quad (22)$$

The result is then written out in terms of the band-energy differences $\Delta e_i(\mathbf{q})$, $i = 0, 1, \dots, 3$:

$$j_{12}(\mathbf{q}) = \left[\Delta e_0(\mathbf{q}) - \frac{1}{2} \sum_{i=1}^2 \Delta e_i(\mathbf{q}) \right] / 2M_1 M_2 \sin^2 \theta, \quad (23)$$

$$j_{11}(\mathbf{q}) = j_{11}(0) + \left[\frac{1}{2} \sum_{i=1}^2 \Delta e_i(\mathbf{q}) - \Delta e_3(\mathbf{q}) + 2M_1 M_2 j_{11}(0) F(\theta) \right] / M_1^2 \sin^2 \theta, \quad (24)$$

and

$$j_{22}(\mathbf{q}) = j_{22}(0) + \left[2M_1 M_2 j_{12}(0) \sin^2 \frac{\theta}{2} + \Delta e_3(\mathbf{q}) \right] / M_2^2 \sin^2 \theta, \quad (25)$$

where

$$F(\theta) = \sin^2 \theta - 2 \sin^2 \frac{\theta}{2}. \quad (26)$$

The exchange eigenvalues are given by the roots of a quadratic equation, i.e.

$$j_{n=1,2} = (j_{11} + j_{22})/2 \pm \sqrt{j_{12}^2 + [(j_{11} - j_{22})/2]^2}, \quad (27)$$

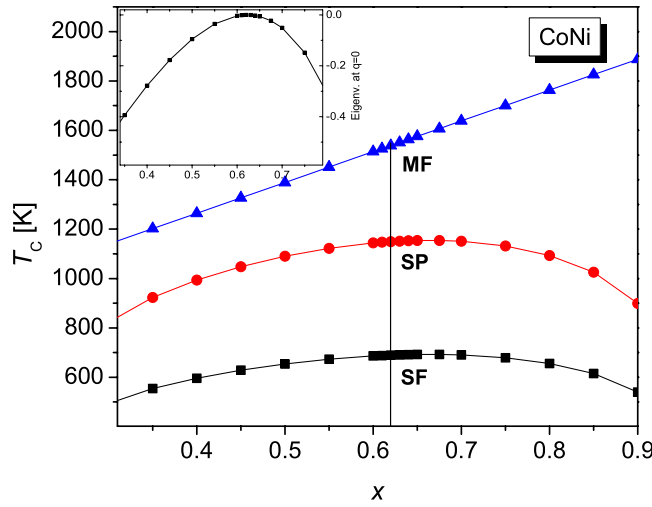


Figure 2. Three approximations for the Curie temperature of CoNi as a function of the interpolation variable x . The curve labelled SF is obtained with the spin-fluctuation choice for the local moments, the curve labelled SP is the spherical approximation, obtained with the local moments equal to the saturation moments at $T = 0$, and the upper curve, MF, gives the mean-field approximation. The inset shows the lowest eigenvalue at $\mathbf{q} = 0$ as a function of x and the vertical line marks the value of x for which the lowest eigenvalue vanishes at $\mathbf{q} = 0$.

(This figure is in colour only in the electronic version)

where, for simplicity in writing, the dependence on \mathbf{q} is implied. The equations (24) and (25) contain the as-yet undetermined coefficients $j_{11}(0)$ and $j_{22}(0)$. Their sum is fixed by

$$M_1^2 j_{11}(0) + M_2^2 j_{22}(0) = \frac{1}{2} \sum_{i=1}^2 e_i(0). \quad (28)$$

Thus one can determine the separate values by interpolating, requiring that the lowest eigenvalue at \mathbf{q} vanishes. The inset of figure 2 gives the lowest eigenvalue at $\mathbf{q} = 0$ as a function of the interpolation variable x . The result of this procedure is seen to be unique and the spherical approximation for the Curie temperature is obtained as $T_c = 1149$ K, which should be compared with the experimental value of $T_c = 1140$ K.

2.3.2. Three magnetic atoms, two being equivalent. An example for this case is the Heusler compound FeSiCo_2 , where the equivalent moments are those of Co. For this case, one must determine the four exchange functions $j_{11}(\mathbf{q})$, $j_{22}(\mathbf{q})$, $j_{12}(\mathbf{q})$, and $j_{23}(\mathbf{q})$ and needs eight scans of the BZ. The discussion is simplified by making a special choice for the angles θ given in table 1, where the reciprocal lattice vectors are also listed to eliminate the cosine term.

The single magnetic moment is denoted with the label 1, and the two equivalent moments with the label 2. Subtracting as before the energy origin

$$e_0(\mathbf{q} = 0) = M_1^2 j_{11}(0) + 2M_2^2 j_{22}(0) + 4M_1 M_2 j_{12}(0) + 2M_2^2 j_{23}(0), \quad (29)$$

one obtains the four exchange functions in terms of the band-energy difference $\Delta e_i(\mathbf{q})$, $i = 0, 1, \dots, 7$:

$$j_{11}(\mathbf{q}) = j_{11}(0) + \left[\frac{1}{4} \sum_{i=1}^4 \Delta e_i(\mathbf{q}) - \frac{1}{2} \sum_{i=5}^6 \Delta e_i(\mathbf{q}) \right] / M_1^2, \quad (30)$$

Table 1. Choice of angles and reciprocal-space vectors \mathbf{q}' for evaluating (21) for the case of three magnetic atoms in the unit cell with two being equivalent. The quantities \mathbf{K}_i are reciprocal lattice vectors ($\mathbf{K}_1 \cdot \boldsymbol{\tau}_{12} = \mathbf{K}_1 \cdot \boldsymbol{\tau}_{13} = \pi$ and $\mathbf{K}_2 \cdot \boldsymbol{\tau}_{23} = \mathbf{K}_3 \cdot \boldsymbol{\tau}_{23} = \pi$). The notation for the band energies is given in the last column.

$\{\mathbf{q}'\}$	θ_1	θ_2	θ_3	$\varphi_1 - \varphi_2$	$\varphi_1 - \varphi_3$	$\varphi_2 - \varphi_3$	Energy
\mathbf{q}	$\pi/2$	$\pi/2$	$\pi/2$	0	0	0	$e_0(\mathbf{q})$
\mathbf{q}	$\pi/2$	$\pi/2$	$\pi/2$	$\mathbf{q}' \cdot \boldsymbol{\tau}_{12}$	$\mathbf{q}' \cdot \boldsymbol{\tau}_{13}$	$\mathbf{q}' \cdot \boldsymbol{\tau}_{23}$	$e_1(\mathbf{q})$
$\mathbf{q} + \mathbf{K}_1$	$\pi/2$	$\pi/2$	$\pi/2$	$\mathbf{q}' \cdot \boldsymbol{\tau}_{12}$	$\mathbf{q}' \cdot \boldsymbol{\tau}_{13}$	$\mathbf{q}' \cdot \boldsymbol{\tau}_{23}$	$e_2(\mathbf{q})$
$\mathbf{q} + \mathbf{K}_2$	$\pi/2$	$\pi/2$	$\pi/2$	$\mathbf{q}' \cdot \boldsymbol{\tau}_{12}$	$\mathbf{q}' \cdot \boldsymbol{\tau}_{13}$	$\mathbf{q}' \cdot \boldsymbol{\tau}_{23}$	$e_3(\mathbf{q})$
$\mathbf{q} + \mathbf{K}_3$	$\pi/2$	$\pi/2$	$\pi/2$	$\mathbf{q}' \cdot \boldsymbol{\tau}_{12}$	$\mathbf{q}' \cdot \boldsymbol{\tau}_{13}$	$\mathbf{q}' \cdot \boldsymbol{\tau}_{23}$	$e_4(\mathbf{q})$
\mathbf{q}	0	$\pi/2$	$\pi/2$	$\mathbf{q}' \cdot \boldsymbol{\tau}_{12}$	$\mathbf{q}' \cdot \boldsymbol{\tau}_{13}$	$\mathbf{q}' \cdot \boldsymbol{\tau}_{23}$	$e_5(\mathbf{q})$
$\mathbf{q} + \mathbf{K}_3$	0	$\pi/2$	$\pi/2$	$\mathbf{q}' \cdot \boldsymbol{\tau}_{12}$	$\mathbf{q}' \cdot \boldsymbol{\tau}_{13}$	$\mathbf{q}' \cdot \boldsymbol{\tau}_{23}$	$e_6(\mathbf{q})$
\mathbf{q}	0	$\pi/2$	$\pi/2$	0	0	0	$e_7(\mathbf{q})$

$$j_{22}(\mathbf{q}) = j_{22}(0) + \left[\frac{1}{2} \sum_{i=5}^6 \Delta e_i(\mathbf{q}) + 4M_1 M_2 j_{12}(0) + 2M_2 j_{23}(0) \right] / 2M_2^2, \quad (31)$$

$$j_{12}(\mathbf{q}) = \left[\Delta e_0(\mathbf{q}) + \frac{1}{2} \sum_{i=5}^6 \Delta e_i(\mathbf{q}) - \Delta e_7(\mathbf{q}) - \frac{1}{4} \sum_{i=1}^4 \Delta e_i(\mathbf{q}) \right] / 4M_1 M_2, \quad (32)$$

and

$$j_{23}(\mathbf{q}) = \left[\Delta e_7(\mathbf{q}) - \frac{1}{2} \sum_{i=5}^6 \Delta e_i(\mathbf{q}) \right] / 2M_2^2. \quad (33)$$

The exchange eigenvalues are given by $j_{n=1} = j_{22} - j_{23}$ and

$$j_{n=2,3} = (j_{11} + j_{22} + j_{23})/2 \pm \sqrt{2j_{12}^2 + [(j_{11} - j_{22} - j_{23})/2]^2}, \quad (34)$$

where, for simplicity in writing, the \mathbf{q} -dependence of the exchange functions is implied.

As before, one sees that (30) and (31) contain the as-yet undetermined coefficients $j_{11}(0)$ and $j_{22}(0)$. Since their sum is fixed by

$$M_1^2 j_{11}(0) + 2M_2^2 j_{22}(0) = \frac{1}{4} \sum_{i=1}^4 e_i(0), \quad (35)$$

one may use the interpolation scheme as before, obtaining again a unique value for the Curie temperature.

2.3.3. Four magnetic atoms, three being equivalent. An example for this case is the Cu_3Au structure, such as, for instance, Ni_3Fe , where the equivalent moments are those of Ni. The single magnetic moment is denoted with the label 1. There are now ten BZ scans needed. For the choice of angles and the notation, one may expand table 1 in an obvious way by two columns and two lines, the latter being added before line seven with reciprocal lattice vectors \mathbf{K}_1 and \mathbf{K}_2 with polar angle $\theta_1 = 0$. For the Cu_3Au structure, \mathbf{K}_1 , \mathbf{K}_2 , and \mathbf{K}_3 are the basis vectors of the simple cubic reciprocal lattice. The derivation of the expressions for the exchange functions in terms of band-energy differences follows the same scheme as in the previous cases, with the following result:

$$j_{11}(\mathbf{q}) = j_{11}(0) + \left[\frac{1}{4} \sum_{i=1}^4 \Delta e_i(\mathbf{q}) - \frac{1}{4} \sum_{i=5}^8 \Delta e_i(\mathbf{q}) \right] / M_1^2, \quad (36)$$

Table 2. Collection of pertinent experimental and calculated data for 11 selected magnetic compounds.

Compound	Lattice	a (Å)	c/a	M_1 (μ_B)	M_2 (μ_B)	T_c^{SP} (K)	T_c^{MF} (K)	T_c^{exp} (K)
FeNi ^a	CuAu	2.481	$\sqrt{2}$	2.551	0.600	972	1130	790
CoNi ^a	CuAu	2.459	$\sqrt{2}$	1.643	0.673	1149	1538	1140
FeNi ₃ ^a	AuCu ₃	3.489		2.822	0.588	986	1290	870
CoNi ₃ ^a	AuCu ₃	3.473		1.640	0.629	733	925	920
NiMnSb ^b	C1 _b	5.920		3.697	0.303	968 ^c	1281	730
Mn ₂ VAI ^d	L2 ₁	5.875		-0.769	1.374	580	663	760
Co ₂ FeSi ^e	L2 ₁	5.640		2.698	1.149	1058	1267	1100
Mn ₃ Al ^f	L2 ₁	5.804		-2.258	1.128	196	342	
Mn ₃ Ga ^f	L2 ₁	5.823		-2.744	1.363	314	482	
Mn ₃ Ga ^f	DO22	3.772	1.898	-2.829	2.273	762	1176	
RhMn ₃ ^g	AuCu ₃	3.800		3.066		1059		855

^a Lattice constants and experimental Curie temperatures from [35].^b Lattice constants and experimental Curie temperatures from [36].^c $T_c^{SP} = 1091$ K if moment of Ni is neglected.^d Lattice constants and experimental Curie temperatures from [38].^e Lattice constant calculated and experimental Curie temperature from [39, 40].^f Lattice constants calculated by [10] and [41].^g Lattice, magnetic structure and Néel temperature from [42].

$$j_{22}(\mathbf{q}) = j_{22}(0) + \left[\frac{1}{4} \sum_{i=5}^8 \Delta e_i(\mathbf{q}) + 6M_1M_2j_{12}(0) + 6M_2j_{23}(0) \right] / 3M_2^2, \quad (37)$$

$$j_{12}(\mathbf{q}) = \left[\Delta e_0(\mathbf{q}) + \frac{1}{4} \sum_{i=5}^8 \Delta e_i(\mathbf{q}) - \Delta e_9(\mathbf{q}) - \frac{1}{4} \sum_{i=1}^4 \Delta e_i(\mathbf{q}) \right] / 4M_1M_2, \quad (38)$$

and

$$j_{23}(\mathbf{q}) = \left[\Delta e_9(\mathbf{q}) - \frac{1}{4} \sum_{i=5}^8 \Delta e_i(\mathbf{q}) \right] / 6M_2^2. \quad (39)$$

Finally, the exchange eigenvalues are given by twice $j_{n=1,2} = j_{22} - j_{23}$ and

$$j_{n=3,4} = (j_{11} + j_{22} + 2j_{23})/2 \pm \sqrt{3j_{12}^2 + [(j_{11} - j_{22} - 2j_{23})/2]^2}, \quad (40)$$

where, for simplicity in writing, the \mathbf{q} -dependence of the exchange functions is implied. The open exchange constants are determined as before.

3. Results and discussion

The reason for the choice of the magnetic compounds listed in table 2 is first the need to establish a certain level of confidence for the numerical procedure employed here. Thus FeNi and CoNi serve as examples for the two-sublattice case given in section 2.3.1. The much-studied Heusler compound NiMnSb can also be treated as a two-sublattice case if one is interested in the role of the small Ni-moment [17]. The classical systems FeNi₃ and CoNi₃ are examples for section 2.3.3, whereas the compounds Mn₂VAI, Co₂FeSi, and Mn₃Ga require the use of the formulae given in section 2.3.2.

The Curie temperature of FeNi is overestimated; recalling that the spin-fluctuation approximation (SFA) (section 2.2) gives $T_c^{SF} = 3/5 \cdot T_c^{SP} = 583$ K, the experimental value is bordered by T_c^{SF} and T_c^{SP} . This is also so for FeNi₃, whereas CoNi is well described by the

spherical approximation (SPA). The Curie temperature of CoNi_3 is underestimated by both the SFA and the SPA, the experimental value being near the mean-field approximation (MFA).

The system NiMnSb is the much-studied half-metallic C1_b -Heusler compound [36]. A previous estimate of the Curie temperature in [37] started out with the SFA, to which a contribution from the dynamic susceptibility was added to obtain agreement with the measured value. The later estimate by Sasioglu *et al* [17] is, with 900 K, close to the value in the SPA. Ignoring the magnetic moment of Ni, a rather high value for T_c^{SP} is obtained, which does not agree with [17]. All in all, the experimental value is again bordered by the SFA (580 K) and the SPA.

The system Mn_2VAl is a half-metallic ferrimagnet for which Weht and Pickett [38] calculated the electronic structure. The calculations underlying the present estimate of the Curie temperature were obtained in the LSDA, i.e. no generalized gradient correction (GGA) was applied as in [38], which resulted in a smaller energy gap here and probably is the reason why the MFA underestimates the experimental Curie temperature. Generally, the MFA supplies an upper bound. The net magnetic moment obtained in the LSDA here is $1.98 \mu_B$, to be compared with the $2 \mu_B$ by [38]. The results give support to the statement of Weht and Pickett [38] that the GGA makes a qualitative difference in the predicted behaviour of Mn_2VAl .

The ferromagnetic Heusler compound Co_2FeSi according to Wurmehl *et al* [39] and Fecher *et al* [40] possesses a very large total magnetic moment of $6 \mu_B$ per formula unit and is half-metallic. The LSDA does not succeed in giving this state, instead it places the Fermi energy above the gap and gives a magnetic moment of about $5 \mu_B$ per formula unit. Apparently, the effects of correlation are so important here that the LSDA+U needs to be employed [40]. It is still somewhat surprising that the SPA for the Curie temperature, with 1057 K, is so close to the measured value 1100 K.

The next three compounds in table 2 motivated the present investigation. These are Heusler compounds like the prototypical Pd_2MnSn , where Mn occupies two different lattice sites: MnI on the Mn-site and MnII on the Pd-sites. They were predicted to be ferrimagnetic and half-metallic, with a nearly zero net moment [10]. The ASW-LSDA calculations performed here for Mn_3Al and Mn_3Ga do give spin polarizations of 96% and 98% at the Fermi energy, respectively, in good agreement with the full-potential calculations of Wurmehl *et al* [10], whose calculated density of states is also in very good agreement with the results shown in figure 3. The estimated Curie temperature for Mn_3Al is likely to be below room temperature, whereas that for Mn_3Ga in the L2_1 structure is definitely higher. Recent measurements show, however, that Mn_3Ga prefers the tetragonal DO22-structure [41], for which indeed the ASW-LSDA calculations show a relative stability by 0.1 eV per formula unit if the lattice constants supplied by Felser and Fecher [41] are used in the calculations. In the DO22-structure, the spin polarization is still of the order of 66% (see figure 3) and the estimated Curie temperature is quite high, with $T_c^{\text{SP}} = 762$ K. This value is correlated with a large increase in the magnetic moment of MnII, labelled M_2 in table 2. When, however, the relative stability of Mn_3Al is checked by total-energy calculations, it is found to be more stable in L2_1 by 0.13 eV per formula unit compared with the DO22-structure. Another structure possible by stoichiometry is AuCu_3 , which may be constructed to be a non-collinear antiferromagnet. It is found to have a Mn-moment of $2.2 \mu_B$ and is unstable by about 0.3 eV per formula unit with respect to the L2_1 structure. It should be emphasized, however, that no lattice optimization was carried out. Since Mn_3Al thus most likely crystallizes in the L2_1 structure, the estimated Curie temperature of about 200 K should be validated experimentally.

The final entry in table 2 concerns RhMn_3 . This is a non-collinear antiferromagnet which has the AuCu_3 structure. The electronic and magnetic properties were described some time ago [42], where the geometry of the non-collinear moment arrangement is also depicted and

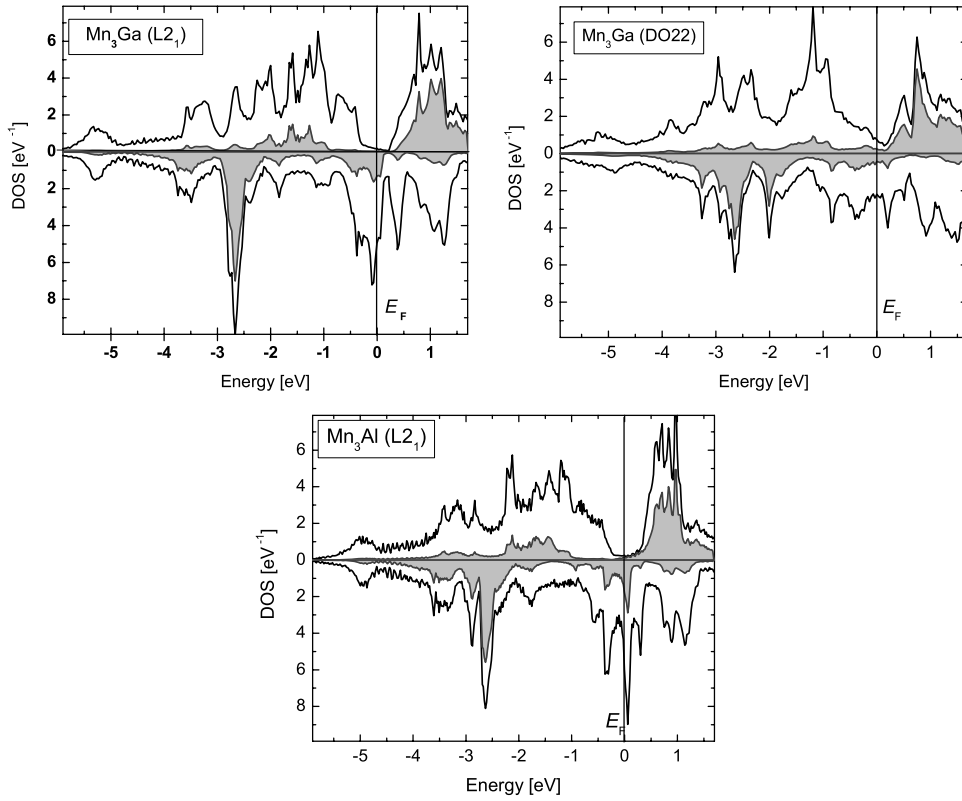


Figure 3. Spin-resolved density of states (DOS) of cubic Mn_3Ga in the L_{21} structure, tetragonal Mn_3Ga in the DO22 structure, and cubic Mn_3Al in the L_{21} structure. The curves bordering the shaded areas are the density of states of the d-electrons of MnI, for which the magnetic moments are given in table 2 as M_I .

references to experimental work are given. The three Mn atoms are equivalent, which requires the evaluation of two exchange functions $j_{11}(\mathbf{q})$ and $j_{12}(\mathbf{q})$ from equation (21), obtaining the angles from figure 5(a) of [42]. The Néel temperature is then calculated in the spherical approximation with equation (18) where the eigenvalues are twice $j_{11}(\mathbf{q}) - j_{12}(\mathbf{q})$ and once $j_{11}(\mathbf{q}) + 2j_{12}(\mathbf{q})$. The SPA is seen to overestimate the experimental Néel temperature of 855 K, which is thus bracketed by the SFA (635 K) and the SPA.

Summary

The central result is equation (18). Although, as it stands, it contains the local moments squared, \mathcal{L}_τ^2 , as unknown quantities, it still allows us to make useful approximations for the Curie or Néel temperature of metallic magnets. It is shown for iron how the unknown value of \mathcal{L}^2 might be approximated, but in all further applications treated here the values of the local moments are taken as the atomic magnetic moments in the ground state. As stressed by Moriya [9], equation (18) covers the range of weak ferromagnets up to the local moment limit. Thus, out of eight metallic magnets studied here, one finds six where the measured Curie (Néel) temperature is in between the spin-fluctuation limit and the spherical approximation limit, in most cases the latter being closer to experiment. Therefore, the predictions by the spherical approximation for the cases where the Curie temperatures are not known are expected to be quite reliable.

Acknowledgments

I am indebted to Claudia Felser for her invitation to the 4th International Symposium on New Materials with High Spin Polarization and for her involving me in exciting physics. I am also grateful to Leonid Sandratskii for many helpful discussions and comments.

References

- [1] Hubbard J 1979 *Phys. Rev. B* **20** 4584
- [2] Fulde P 1991 *Electron Correlations in Molecules and Solids* (Berlin: Springer)
- [3] Staunton J B 1994 *Rep. Prog. Phys.* **57** 1289
- [4] Lichtenstein A I, Katsnelson M I and Kotliar G 2001 *Phys. Rev. Lett.* **87** 067205
- [5] Rhodes P and Wohlfarth E P 1963 *Proc. R. Soc. A* **273** 247
- [6] Lonzarich G G and Taillefer L 1985 *J. Phys. C: Solid State Phys.* **18** 4339
- [7] Mohn P 2003 *Magnetism in the Solid State: an Introduction* (Berlin: Springer)
- [8] Kübler J 2004 *Phys. Rev. B* **70** 064427
- [9] Moriya T 1985 *Spin Fluctuations in Itinerant Electron Magnetism* (Berlin: Springer) chapters 7, 8
- [10] Wurmehl S, Kandpal H C, Fecher G H and Felser C 2006 *J. Phys.: Condens. Matter* **18** 6171
- [11] Ishikawa Y 1977 *Physica B* **91** 130
- [12] Kübler J, Williams A R and Sommers C B 1983 *Phys. Rev. B* **28** 1745
- [13] Kohn W and Sham L J 1965 *Phys. Rev.* **140** A1133
- [14] Uhl M and Kübler J 1996 *Phys. Rev. Lett.* **77** 334
- [15] Sandratskii L M 1998 *Adv. Phys.* **47** 91
- [16] Halilov S V, Eschrig H, Perlov A Y and Oppeneer P M 1998 *Phys. Rev. B* **58** 293
- [17] Sasioglu E, Sandratskii L M, Bruno P and Galanakis I 2005 *Phys. Rev. B* **72** 184415
- [18] Herring C 1966 *Magnetism* vol 4, ed G Rado and H Suhl (New York: Academic) chapters V and XIII
- [19] Sandratskii L M 1986 *J. Phys. F: Met. Phys.* **16** L43
- [20] Niu Q and Kleinman L 1998 *Phys. Rev. Lett.* **80** 2205
- [21] Niu Q, Wang X, Kleinman L, Liu W-M, Nicholson D M C and Stocks G M 1999 *Phys. Rev. Lett.* **83** 207
- [22] Moriya T and Takahashi Y 1978 *J. Phys. Soc. Japan* **45** 397
- [23] Tahir-Keli R A and ter Haar D 1962 *Phys. Rev.* **127** 88
- [24] Tahir-Keli R A and Jarrett H S 1964 *Phys. Rev.* **135** A1096
- [25] Tyablikov S V 1967 *Methods in Quantum Theory of Magnetism* (New York: Plenum)
- [26] Schwarz K and Mohn P 1984 *J. Phys. F: Met. Phys.* **14** L129
- [27] Kübler J 2000 *Theory of Itinerant Electron Magnetism* (Oxford: Clarendon)
- [28] Kübler J 2007 *The Handbook of Modern Magnetism and Advanced Magnetic Materials* vol 1, ed H Kronmüller and S Parkin (London: Wiley)
- [29] Shimizu M 1981 *Rep. Prog. Phys.* **44** 329
- [30] Anderson P W 1955 *Solid State Physics* vol 14, ed F Seitz and D Turnbull (New York: Academic) pp 99–214
- [31] Heine V 1980 *Solid State Physics* vol 35, ed H Ehrenreich, F Seitz and P Turnbull (New York: Academic)
- [32] Mackintosh A R and Andersen O K 1980 *Electrons at the Fermi Surface* ed M Springford (Cambridge: Cambridge University Press) p 149
- [33] Williams A R, Kübler J and Gelatt C D 1979 *Phys. Rev. B* **19** 6094
- [34] von Barth U and Hedin L 1972 *J. Phys. C: Solid State Phys.* **5** 1629
- [35] Bonnenberg D, Hempel K A and Wijn H P J 1986 *Landolt-Börnstein, New Series III/19a* ed K-H Hellwege (Berlin: Springer) chapter 1.2.1
- [36] de Groot R A, Mueller F M, van Engen P G and Buschow K H J 1983 *Phys. Rev. Lett.* **50** 2024
- [37] Kübler J 2003 *Phys. Rev. B* **67** 220403
- [38] Weht R and Pickett W E 1999 *Phys. Rev. B* **60** 13006
- [39] Wurmehl S, Fecher G H, Kandpal H C, Ksenofontov V, Fecher C, Lin H-J and Morais J 2005 *Phys. Rev. B* **72** 184432
- [40] Fecher G H, Kandpal H C, Wurmehl S, Felser C and Schönhense G 2006 *Appl. Phys.* **99** 08J106
- [41] Felser C and Fecher G H 2006 private communication
- [42] Kübler J, Höck K-H, Sticht J and Williams A R 1988 *J. Phys. F: Met. Phys.* **18** 469